ArHg⁺-Ions in the Mercury-Argon Low Pressure Discharge — Mass Spectrometric Analysis of the Formation Process

Günter Franck

OSRAM-Studiengesellschaft München

(Z. Naturforsch. **28 a**, 1481—1488 [1973]; received 20 March 1973)

The ion components of the mercury argon low pressure discharge are analysed with help of a quadrupole mass spectrometer. Here we have found besides the main components Hg^+ and Ar^+ the diatomic ion-molecules Hg_2^+, Ar_2^+ and $ArHg^+$. With a discharge current of 200 mA, argon pressure 0,2 torr and mercury vapour pressure $2.8 \cdot 10^{-3}$ torr, the ion components are in the ratio

$$[Hg^+] : [Ar^+] : [ArHg^+] : [Hg_2^+] : [Ar_2^+] = 1000 : 134 : 24 : 10 : 3 .$$

The ratios $i(ArHg^+)/i(Ar_2^+)$, $i(Ar^+)/i(Hg^+)$, $i(Ar_2^+)/i(Ar^+)$, $i(Hg_2^+)/i(Hg^+)$ of the effusing ion currents are measured as a function of mercury vapor pressure, discharge current and argon pressure. These measurements yield the following formation processes of $ArHg^+$ and Ar_2^+:

$$Ar^m + Hg \xrightarrow{k^{ArHg^+}} ArHg^+ + e, \quad (Ar^m: \text{ metastable, } E > 11.5 \text{ eV}),$$

$$Ar^* + Ar \xrightarrow{k^{Ar_2^+}} Ar_2^+ + e, \quad (Ar^*: \text{ highly excited, } E > 14.7 \text{ eV}).$$

For the products of reaction rates k and lifetimes τ^{Ar^m}, τ^{Ar^*} of the metastable and highly excited Ar-atoms, we get

$$k^{ArHg^+} \cdot \tau^{Ar^m} = 61 \cdot 10^{-16} \text{ cm}^3,$$
$$k^{Ar_2^+} \cdot \tau^{Ar^*} = 1.1 \cdot 10^{-16} \text{ cm}^3 .$$

So the following cross sections are found:

$$\sigma^{ArHg^+} = 5.8 \cdot 10^{-15} \text{ cm}^2,$$
$$\sigma^{Ar_2^+} = 3.6 \cdot 10^{-15} \text{ cm} .$$

In an earlier work[1] we have reported a mass spectrometric analysis of Hg_2^+-formation in the positive column of the Hg-Ar low pressure discharge. There, we identified the process of associative ionization as the dominant Hg_2^+-formation mechanism:

$$\left.\begin{matrix} Hg\,(^3P_0) \\ Hg\,(^3P_1) \\ Hg\,(^3P_2) \end{matrix}\right\} + \left\{\begin{matrix} Hg\,(^3P_1) \\ Hg\,(^3P_2) \end{matrix}\right. \rightarrow Hg_2^+ + e . \qquad (1)$$

In addition to the Hg_2^+-ion we have found under certain discharge conditions the ions Ar_2^+ and the $ArHg^+$. The latter had not been identified before in discharges. The aim of the present experiments was to determine the formation process of Ar_2^+ and $ArHg^+$ and the corresponding cross sections.

I. Rare gas ion-molecules

Mass spectrometric analysis of stationary low pressure discharges is well suited to demonstrate the formation of molecular ions, by both new processes and by processes already known from experiments with ionization chambers (see e.g. [2–9]). For example, in rare gas discharges [10–13] the ions He_2^+, Ne_2^+, Ar_2^+ are found which are formed by the Hornbeck-Molnar process[14]

$$X^* + X \rightarrow X_2^+ + e \qquad (2)$$

(X^* highly excited rare gas atoms He, Ne, Ar, Kr, Xe).

In rare gas mixtures of He + Ne, Pahl and Weimer[15] identified the $HeNe^+$-ion and established the process

$$He^* + Ne \rightarrow HeNe^+ + e . \qquad (3)$$

Later experiments with ionization chambers[2,16,17] yielded further heteronuclear rare gas ion-molecules $NeAr^+$, $ArKr^+$, $KrXe^+$, $HeAr^+$.

In Ar-discharges with an admixture of hydrogen, Pahl[18] and Knewstubb and Tickner [12] observed the ArH^+-ion. It is formed (see [18]) by the reaction

$$Ar^m + H \rightarrow ArH^+ + e \qquad (4)$$

(Ar^m metastable Ar-atom, $E(Ar^m) = 11{,}55$ or 11,71 eV).

Reprint requests to Dr. G. Franck, OSRAM GmbH, *D-8000 München 90*, Postfach 90 06 20.

Further rare gas (X)-hydrogen systems have been studied in the ionization chamber[19–28]. Here, the reactions are mainly of the type

$$X^+ + H_2 \rightarrow XH^+ + H \qquad (5)$$

$$X + H_2^+ \rightarrow XH^+ + H\,. \qquad (6)$$

In rf-discharges in Ar + Cs Gilkinson, Held and Chanin[29] under certain discharge conditions observed the $ArCs^+$-ion. Herman and Čermák[30] have also discovered this ion in ionization chamber experiments in mixtures of rare gas (X) and alkali metal vapors (Me). In this work, reactions in the mixtures of mercury vapor with noble gases were also studied. The ions $ArHg^+$, $KrHg^+$ and $XeHg^+$ have been found, but not the ions $NeHg^+$ and $HeHg^+$. According to [30], the appearance potentials of the ion-molecules XMe^+ correspond to the well known metastable states of the rare gas atoms. So all reactions are of the type

$$X^m + Me \rightarrow XMe^+ + e\,. \qquad (7)$$

Probably these reactions are concurring with reactions of the type

$$X^m + Me \rightarrow Me^+ + X + e\,. \qquad (8)$$

Other types of rare gas molecular ions have been found only in the ionization chamber. For exampel, in rare gas-N_2 and rare gas-CO mixtures[31] the ions XC^+, XN^+, XN_2^+, XCO^+ (X = Ar, Kr, Xe) were observed.

Henglein and Muccini[32] report about the ArJ^+ and KrJ^+-ion. The appearance potential of ArJ^+ is equal to the excitation potential (11,5 eV) of $Ar(^3P_2)$. The reaction

$$Ar(^3P_2) + J_2 \rightarrow ArJ^+ + J + e \qquad (9)$$

is exothermic as shown in [32], whereas the reaction

$$Ar(^3P_2) + J_2 \rightarrow Ar + J^+ + J + e \qquad (10)$$

is endothermic. The appearance potential of KrJ^+ lies about 0.6 eV below the ionization potential of krypton (14.0 eV), whereas the metastable $Kr(^3P_2)$ with 9.91 eV does not lead to an exothermic reaction according to (9).

The determination of the formation mechanism of the $ArHg^+$- and Ar_2^+-ions, which we have observed besides the ions Hg^+, Ar^+, and Hg_2^+ required first an investigation of the dependence of $ArHg^+$ and Ar_2^+ on the discharge parameters: mercury pressure p_{Hg}, discharge current i_d and argon pressure p_{Ar}.

II. Experimental

The experimental arrangement (Fig. 1) is nearly the same as in [1]: A U-shaped discharge vessel (Pyrex, $\varnothing_i = 10$ mm) projects into an UHV-recipient, where — opposite the discharge — the quadrupole mass spectrometer is located. The extraction probe (S) in the wall of the discharge vessel is a 27 μ thick molybdenum sheet with five holes of 20 μ diameter. The potential of the extraction probe can be varied with respect to the plasma potential, but in our case the extraction probe is always held on floating potential, when the ions are effusing into the mass spectrometer. The distance between

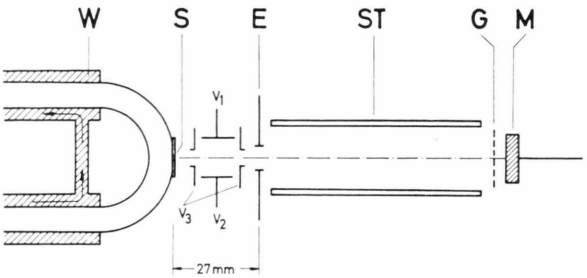

Fig. 1. Experimental arrangement. W: water jacket, S: ion extraction probe, E: entrance aperture of the quadrupole, ST: rod system, G: grid, M: multiplier.

the extraction probe and the grounded entrance aperture of the mass spectrometer is 27 mm. The effusing ion current can be maximized by the potentials V_1, V_2 of two deflecting plates and by a focussing lens (V_3).

The mercury vapor pressure in the discharge is regulated by a thermostatically controlled jacket surrounding the discharge vessel. With the being in operation, the temperatures of the nonthermostated parts of the vessel (electrode ends, effusion probe) are always higher than the temperatures of the thermostat, so that the Hg-vapor pressure is not falsified.

At a rare gas pressure of 1 torr in the discharge, the pressure in the UHV-recipient is nearly 10^{-6} torr.

III. Results

Variation of mercury vapor pressure

In Fig. 2 the ion current ratios $i(ArHg^+)/i(Ar_2^+)$, $i(Ar^+)/i(Hg^+)$, $i(Ar_2^+)/i(Ar^+)$ and $i(Hg_2^+)/i(Hg^+)$ are shown as a function of p_{Hg} with constant discharge current and argon pressure. $i(ArHg^+)/i(Ar_2^+)$ increases proportionally with p_{Hg} for $p_{Hg} < 0.01$ torr, whereas $i(Ar^+)/i(Hg^+)$ is nearly proportional to $1/p_{Hg}$. At very low mercury vapor pressures, $i(Ar^+)$

and $i(Hg^+)$ are nearly equal. — $i(Ar_2^+)/i(Ar^+)$ does not vary with p_{Hg}. Therefore Hg-atoms evidently do not play a role in the Ar_2^+-formation. — $i(Hg_2^+)/i(Hg^+)$ is increasing nearly proportional to p_{Hg}. That can be explained by the fact, that (see [1]) $[Hg_2^+]$ is proportional to p_{Hg}^2, whereas [Hg] is proportional to p_{Hg}.

Variation of discharge current

The ratio $i(ArHg^+)/i(Ar_2^+)$ is roughly independent of i_d. Whereas when $i_d \geqq 20$ mA, $i(Ar^+)/i(Hg^+)$ increases proportional to i_d and $i(Ar_2^+)/i(Ar^+)$ decreases proportional to $1/i_d$. In a similar way $i(Hg_2^+)/i(Hg^+)$ decreases with $1/i_d$ for $i_d > 40$ mA.

When $i_d = 200$ mA, $p_{Ar} = 0{,}2$ torr, $p_{Hg} = 2{,}8 \cdot 10^{-3}$ torr, the ion currents in the mass spectrometer are found to be in the ratios

$$i(Hg^+) : i(Ar^+) : i(ArHg^+) : i(Hg^+) : i(Ar_2^+) = 1000 : 300 : 22 : 7.5 : 5 .$$

The ion densities and the effusion ion currents are related via

$$\frac{A^+}{B^+} = \frac{i(A^+)}{i(B^+)} \cdot \sqrt{\frac{M(A)}{M(B)}}, \qquad (11)$$

where A^+ and B^+ are any ions and $M(A)$ and $M(B)$ their respectively molecular weights. Accordings by we obtain for the ratios of the ion densities

$$[Hg^+] : [Ar^+] : [ArHg^+] : [Hg_2^+] : [Ar_2^+] = 1000 : 134 : 24 : 10.5 : 3.1 .$$

As shown in [33,34] and according to our measurements, the Hg^+-concentration in the Hg-Ar-column increases linearly with the discharge current i_d. Therefore, for $i_d > 20$ mA the Ar^+-concentration must grow with i_d^2 or n_e^2 respectively. Here the ionization of argon takes place — as also supposed by Wojaczek[35] — via an intermediate level or more narrow neighbouring levels, whose population density increases linearly with i_d.

According to Fig. 2 the concentration of Ar_2^+ increases proportional to i_d in the same way as the $ArHg^+$-concentration.

As the ratio $i(Hg_2^+)/i(Hg^+)$ is inversely proportional and $i(Hg^+)$ proportional to i_d when $i_d > 40$ mA, Hg_2^+ must then be independent of the discharge current. This result was found already in [1]. As shown there, the population densities of the metastable levels $Hg(^3P_0)$ and $Hg(^3P_2)$, which are responsible for the Hg_2^+-formation, do not increase with the discharge current for $i_d > 40$ mA. (That is apparent also from the optically measured population densities of Koedam and Kruithof[36]). Population by electron excitation and depopulation by electron collisions of the second kind are in equilibrium for $i_d > 40$ mA.

Variation of argon pressure

Figure 2 shows the ion current ratios versus p_{Ar}. The parameters p_{Hg} and i_d are held constant: $i(ArHg^+)/i(Ar_2^+)$ and $i(Ar^+)/i(Hg^+)$ decrease with p_{Ar}. On the other hand, $i(Ar_2^+)/i(Ar^+)$ increases

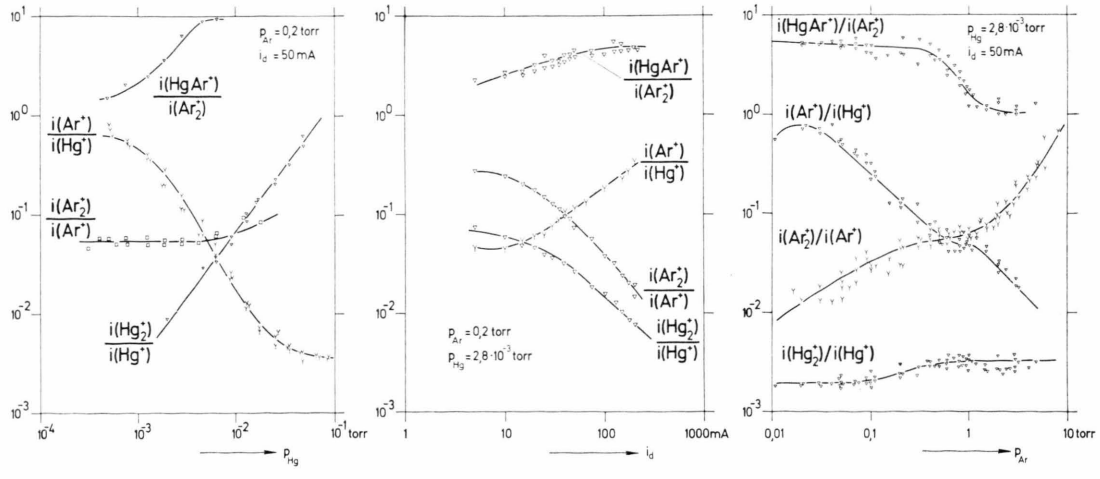

Fig. 2. The measured ion current ratios in the mercury arg discharge as a function of mercury pressure, discharge current and argon pressure.

with p_{Ar}. In the pressure range of 0.01 to 10 torr the slope is not constant. — $i(Hg_2^+)/i(Hg^+)$ is scarcely varying with the argon pressure. This observation indicates, that argon atoms play no role in the Hg_2^+-formation.

IV. The $ArHg^+$-Formation Process

The processes (7) found by Herman and Čermák[30], and the formation process (9) for the ArJ^+-ion found by Henglein and Muccini[32] suggest the following formation process for the $ArHg^+$-formation:

$$Ar^m + Hg \rightarrow ArHg^+ + e\,, \qquad (12)$$

where Ar^m is metastable. This process is exothermic, if

$$E(Ar^m) > E_{ion}(Hg) - E_{diss}(ArHg^+)\,, \qquad (13)$$

where $E(Ar^m)$ is the excitation energy of the metastable Ar, $E_{ion}(Hg)$ ionization energy of Hg and $E_{diss}(ArHg^+)$ dissoziation energy of $ArHg^+$.

In Fig. 3 these energy relations are shown for the rare gases Ne, Ar, Kr, Xe. Except for xenon, the excitation energies of the lowest metastable levels

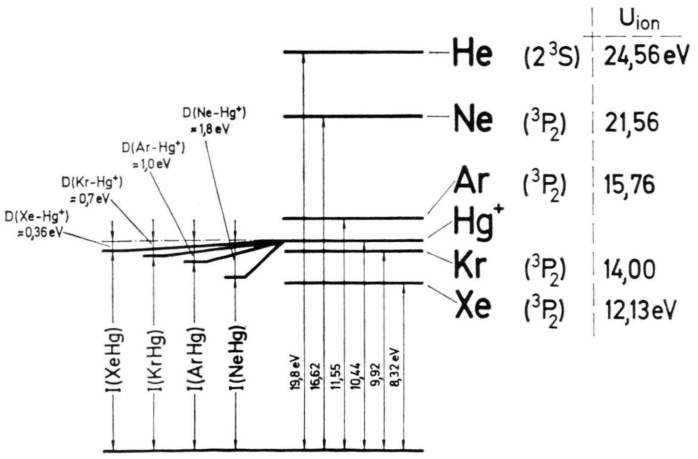

Fig. 3. Energy relations for the mercury-rare gas ion formation by collisions of neutral Hg-atoms with metastable excited rare gas atoms. The dissoziation energies of the mercury-rare gas ions have been equated to the isoelectronic neutral molecules. I are the ionization energies.

of the rare gases are higher than the difference of the ionization energy of Hg and dissoziation energy of the mercury-rare gas ion-molecules. These dissoziation energies of $NeHg^+$, $ArHg^+$, $KrHg^+$ and $XeHg^+$ are assumed equal to the dissoziation energies of the corresponding isoelectronic molecules HgF, HgCl, HgBr, and HgJ, which are well known from[36]. For the $HeHg^+$-ion we find by extrapolation of the binding energies against the atomic number: $E_{diss}(HeHg^+) \approx 1.4$ eV. So, for all rare gases except Xe an exothermic reaction of the type (12) can take place with the excitation of the rare gas atoms corresponding to the lowest metastable states.

Regarding the Ar_2^+-formation process, we expect in the mercury-argon discharge the same formation mechanism as in the discharge of pure argon[18]. Here the Hornbeck-Molnar process (2) leads to the Ar_2^+-ion. Becker and Lampe[7] have shown, that the process (2) in argon takes place mainly via three excited states. The radiation lifetimes of Ar* are 0.77, 0.55 and 0.33 μsec. — By photoionisation measurements Huffman and Katayama[38] could verify, that all optically allowed states above the excitation energy of 14.710 ± 0.009 eV can produce Ar_2^+-ions by the Hornbeck-Molnar process (2).

Making use of these formation processes and the observation that Ar^+ is proportional to n_e (for $i_d < 20$ mA) or proportional to n_e^2 (for $i_d \geqq 20$ mA), we lay down the following collision scheme:

$$Ar + e \xrightarrow{S^{Ar}_{0\infty}} Ar^+ + 2e\,, \quad [i_d < 20\,mA]\,, \qquad (14)$$

$$Ar + e \xrightarrow{S^{Ar}_{0*}} Ar^* + e\,, \quad [E(Ar^*) \geqq 14.7\,eV]\,, \qquad (15)$$

$$Ar^* + Ar \xrightarrow{k^{Ar_2^+}} Ar_2^+ + e\,, \qquad (16)$$

$$Ar + e \underset{\bar{S}^{Ar}_{m0}}{\overset{S^{Ar}_{0m}}{\rightleftarrows}} Ar^m + e\,, \quad [Ar^m \geqq 11.5\,eV]\,, \qquad (17)$$

$$Ar^m + e \xrightarrow{S^{Ar}_{m\infty}} Ar^+ + 2e\,, \quad [i_d > 20\,mA] \qquad (18)$$

$$Ar^m + Hg \xrightarrow{k^{ArHg^+}} ArHg^+ + e\,. \qquad (19)$$

Because of the high effective lifetime of Ar^m, Wojaczek[35] takes into consideration the metastable terms $^3P_0$, $^3P_2$ and the resonance levels $^3P_1$, $^1P_1$. All levels are combined to one excited state Ar^m with the effective excitation energy of 11.5 eV. — In our reaction scheme we suppose, that both the stepwise ionization of Ar, and the $ArHg^+$-formation according to (12) happens via the Ar^m-state. S and k are the electron excitation rates and reaction rates (cm^3/s) respectively.

With the lifetimes τ^{Ar^m}, τ^{Ar^*} of the Ar^m and the highly excited Ar*, and with the diffusion lifetimes $\tau_{diff}^{Ar_2^+}$ and $\tau_{diff}^{ArHg^+}$ of the Ar_2^+- and $ArHg^+$-ions, we obtain by equating loss- and generation processes

the following relation:

$$\frac{[Ar_2^+]}{[ArHg^+]} = \frac{S_{0*}^{Ar}}{S_{0m}^{Ar}} \cdot \left(1 + \frac{1}{\tau^{Ar^m} \cdot k^{ArHg^+} \cdot [Hg]}\right) \cdot \frac{\tau^{Ar^*} \cdot k^{Ar_2^+} \cdot [Ar]}{1 + \tau^{Ar^*} \cdot k^{Ar_2^+} \cdot [Ar]} \cdot \left(1 + \frac{n_e (S_{m\infty}^{Ar} + \bar{S}_{m0}^{Ar}) \cdot \tau^{Ar^m}}{1 + \tau^{Ar^m} \cdot k^{ArHg^+} \cdot [Hg]}\right) \cdot \frac{\tau_{diff}^{Ar_2^+}}{\tau_{diff}^{ArHg^+}} \cdot \quad (20)$$

As is shown in Fig. 2, $i(Ar_2^+)/i(ArHg^+)$ is nearly independent of the discharge current i_d or electron density n_e respectively. Therefore in (20) the following inequality must be fulfilled:

$$n_e (S_{m\infty}^{Ar} + \bar{S}_{m0}^{Ar}) \ll (1/\tau^{Ar^m}) + k^{ArHg^+} \cdot [Hg] . \quad (21)$$

That means that the depopulation of Ar^m by optical transitions plus $ArHg^+$-formation is greater than the depopulation by electron collisions. This result (21) follows also from the observation, that Ar^+ is increasing with i_d^2 or n_e^2 for $i_d \geqq 20$ mA. This functional relation is only possible, if Ar^m is growing linearly with n_e. For $[Ar^m]$ we find with (17), (18), (19)

$$[Ar^m] = \frac{n_e S_{0m}^{Ar} \cdot [Ar]}{(1/\tau^{Ar^m}) + k^{ArHg^+} \cdot [Hg] + n_e (S_{m\infty}^{Ar} + \bar{S}_{m0}^{Ar})} \cdot \quad (22)$$

Thus, $[Ar^m]$ is only increasing proportional with n_e, if the inequality (21) is fulfilled.

For the Ar^m-lifetimes Wojeczek[35] calculates $\tau^{Ar^m} \approx 10^{-5}$ sec. Then, if we assume a collision rate $\bar{S}_{m0}^{Ar}$, $S_{m\infty}^{Ar}$ of about 10^{-7} cm³/s and a plasma density of about 10^{11} cm^{-3} (see [33, 34]), (21) is valid. With (21) we obtain

$$\frac{[Ar_2^+]}{[ArHg^+]} = \frac{S_{0*}^{Ar}}{S_{0m}^{Ar}} \cdot \left(1 + \frac{1}{\tau^{Ar^m} \cdot k^{ArHg^+} \cdot [Hg]}\right) \cdot \frac{\tau^{Ar^*} \cdot k^{Ar_2^+} \cdot [Ar]}{1 + \tau^{Ar^*} \cdot k^{Ar_2^+} \cdot [Ar]} \cdot \frac{\tau_{diff}^{Ar_2^+}}{\tau_{diff}^{ArHg^+}} \cdot \quad (23)$$

If the ratio of ion currents, $y = i(Ar_2^+)/i(ArHg^+)$ is plotted against $1/p_{Hg}$ at constant argon pressure and discharge current, there must result a straight line, if (23) is valid and if it can be assumed, that the point of intersection with the y-axis,

$$y_0 = \sqrt{\frac{240}{80}} \cdot \frac{S_{0*}^{Ar}}{S_{0m}^{Ar}} \cdot \frac{\tau^{Ar*} \cdot k^{Ar_2+} \cdot [Ar]}{1 + \tau^{Ar^*} \cdot k^{Ar_2^+} \cdot [Ar]} \cdot \frac{\tau_{diff}^{Ar_2^+}}{\tau_{diff}^{ArHg^+}} , \quad (24)$$

is independent on p_{Hg}. Denoting the slope by $\mathrm{tg}\alpha$, it follows that the product of Ar^m-lifetime and reaction rate constant of the $ArHg^+$-formation process is

$$\tau^{Ar^m} \cdot k^{ArHg^+} = y_0 / N_1 \,\mathrm{tg}\,\alpha \quad [\mathrm{cm}^3] , \quad (25)$$

where N_1 is the Hg-concentration at $p_{Hg} = 1$ torr.

Figure 4 shows the variation of $i(Ar_2^+)/i(ArHg^+)$ with $1/p_{Hg}$. The evaluation according to (25) yields

$$\tau^{Ar^m} \cdot k^{ArHg^+} = 61.4 \cdot 10^{-16} \,\mathrm{cm}^3 . \quad (26)$$

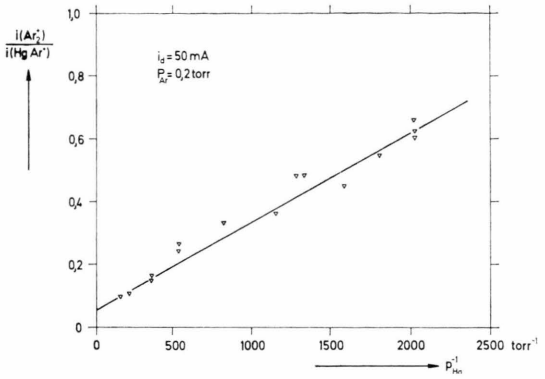

Fig. 4. Variation of $i(Ar_2^+)/i(ArHg^+)$ with the reciprocal mercury presusre $1/p_{Hg}$.

Wojaczek[35] has calculated the lifetimes of the resonance levels $^1P_1$ and $^3P_1$ for the case of Doppler broadening and finds

$$\tau^{Ar^m} = 2.2 \cdot 10^{-4} \cdot R\, p_{Ar} \,[\mathrm{sec}] , \quad (27)$$

where R is the radius of the discharge vessel in cm. So, with (26), the reaction rate constant for the $ArHg^+$-formation process (12) is

$$k^{ArHg^+} = 2.8 \cdot 10^{-10} \,[\mathrm{cm}^3/\mathrm{s}] \quad (28)$$

and the corresponding cross section is

$$\sigma^{ArHg^+} = \frac{k^{ArHg^+}}{\sqrt{\frac{8\,k\,T_g}{\pi} \cdot \left(\frac{1}{M_{Ar}} + \frac{1}{M_{Hg}}\right)}} = \frac{k^{ArHg^+}}{v_{rel}} = \pi (r^{Ar^m} + r^{Hg})^2 = 5.8 \cdot 10^{-15} \,\mathrm{cm}^2 . \quad (29)$$

v_{rel} is the relative velocity of Ar and Hg, r^{Ar^m} and r^{Hg} are the collision radii of Ar^m and Hg.

From (29) we get $r^{Ar^m} + r^{Hg} = 4.3$ Å. Compared with this result, the sum of the corresponding atomic radii[39] is $r^{Ar} + r^{Hg}$ 1.7 Å + 2.2 Å = 3.9 Å.

V. The Ar_2^+-Formation Process

A similar procedure as for the $k\tau$-evaluation of the $ArHg^+$-formation process can be carried out for the Ar_2^+-formation process, too. With the reaction scheme (14)—(19) we get:

$$\frac{[Ar^+]}{[Ar_2^+]} = \frac{S_{0\infty}^{Ar}}{S_{0*}^{Ar}} \cdot \left(1 + \frac{1}{\tau^{Ar^*} \cdot k^{Ar_2^+} \cdot [Ar]}\right) \cdot \left(1 + \frac{n_e S_{0m}^{Ar} S_{m\infty}^{Ar}}{S_{0\infty}^{Ar}} \cdot \frac{1}{(1/\tau\ Ar^m) + [Hg] \cdot k^{ArHg^+} + n_e (S_{m\infty}^{Ar} + \bar{S}_{m0}^{Ar})}\right) \frac{\tau_{diff}^{Ar^+}}{\tau_{diff}^{Ar_2^+}}. \quad (30)$$

Since the stepwise ionization of Ar can be neglected against direct ionization for discharge currents $i_d < 20$ mA, we find from (30)

$$\frac{[Ar^+]}{[Ar_2^+]} = \frac{S_{0\infty}^{Ar}}{S_{0*}^{Ar}} \cdot \left(1 + \frac{1}{\tau^{Ar^*} \cdot k^{Ar_2^+} \cdot [Ar]}\right) \cdot \frac{\tau_{diff}^{Ar^+}}{\tau_{diff}^{Ar_2^+}}; \quad [i_d < 20\ mA]. \quad (31)$$

In Fig. 5 the ratio $i(Ar^+)/i(Ar_2^+)$ is plotted against $1/p_{Ar}$. The discharge current is 10 mA. According to (31) we find a straight line. With the same evaluation procedure as in Fig. 4 we obtain

$$\tau^{Ar^*} \cdot k^{Ar_2^+} = 1.1 \cdot 10^{-16}\ cm^3. \quad (32)$$

As the mean value for the radiation lifetime of Ar* measured by Becker and Lampe [7] is $\tau^{Ar*} \approx 0.5 \cdot 10^{-6}$ s, the reaction rate constant becomes

$$k^{Ar_2^+} = 2.2 \cdot 10^{-10}\ cm^3/s. \quad (33)$$

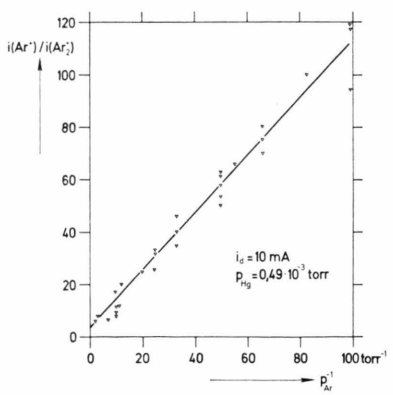

Fig. 5. Variation of $i(Ar^+)/i(Ar_2^+)$ with the reciprocal argon pressure $1/p_{Ar}$.

The corresponding cross section of the Hornbeck-Molnar process (16) is then

$$\sigma^{Ar_2^+} = \pi (r^{Ar^*} + r^{Ar})^2 = 3.6 \cdot 10^{-15}\ cm^2. \quad (34)$$

With (34) we calculate $r^{Ar^*} + r^{Ar} = 3.4$ Å. Compared to it, the sum of the radii of the unexited argon atoms [39] is 3,4 Å.

In discharges of pure argon, Pahl [18] has measured the value $k^{Ar_2^+} \cdot \tau^{Ar*} = 0.84 \cdot 10^{16}$ cm^3. The approximate agreement with our result (32) indicates the same formation mechanism in the Hg-Ar-discharge as in the discharge of pure argon.

In the following table the $k^{Ar_2^+} \cdot \tau^{Ar*}$-values which have been found under different experimental conditions are assembled.

Tab. 1. The $\tau^{Ar^*} \cdot k^{Ar_2^+}$-values found under different experimental conditions.

$\tau^{Ar^*} \cdot k^{Ar_2^+}$ [cm^3]	Method	Reference
$3.6 \cdot 10^{-18} - 1.3 \cdot 10^{-16}$	photon absorption	R. E. Huffman, D. H. Katayama [38]
$4.3 \cdot 10^{-16} - 1.3 \cdot 10^{-15}$	pulsed mass spectrometer	P. M. Becker, F. W. Lampe [7]
$3.6 \cdot 10^{-16}$	ionization chamber	J. S. Dahler, J. L. Franklin, M. S. B. Munson, F. H. Field [4]
$0.83 \cdot 10^{-16}$	ionization chamber	R. Fuchs, W. Kaul [2]
$0.84 \cdot 10^{-16}$	positive column in argon	M. Pahl [18]
$1.1 \cdot 10^{-16}$	positive column in mercury-argon mixtures	this work

Discussion

The dependence of $i(Hg_2^+)/i(Hg^+)$ on the discharge parameters p_{Hg}, i_d, and p_{Ar} and the resulting Hg_2^+-formation process have been discussed previously [1].

Interpretation of the other ion current ratios of Fig. 2, follows the reaction scheme for Hg^+:

$$Hg + e \xrightarrow{S_{0\infty}^{Hg}} Hg^+ + e, \quad (35)$$

$$\mathrm{Hg} + \mathrm{e} \underset{\bar{S}^{\mathrm{Hg}}_{\mathrm{m}0}}{\overset{S^{\mathrm{Hg}}_{0\mathrm{m}}}{\rightleftarrows}} \mathrm{Hg^m} + \mathrm{e}\,, \tag{36}$$

$$\mathrm{Hg^m} + \mathrm{e} \xrightarrow{S^{\mathrm{Hg}}_{\mathrm{m}\infty}} \mathrm{Hg^+} + 2\,\mathrm{e}\,, \tag{37}$$

where $\mathrm{Hg^m} = \mathrm{Hg}(^3\mathrm{P}_0)$, $\mathrm{Hg}(^3\mathrm{P}_1)$, $\mathrm{Hg}(^3\mathrm{P}_2)$ (see[36]).

With $\tau^{\mathrm{Hg^m}}$ as the combined radiation- and diffusion lifetime of $\mathrm{Hg^m}$, we get from (35)—(37)

$$[\mathrm{Hg^+}] = n_\mathrm{e} \cdot [\mathrm{Hg}] \cdot \left(S^{\mathrm{Hg}}_{0\infty} + \frac{n_\mathrm{e} S^{\mathrm{Hg}}_{0\mathrm{m}} \cdot S^{\mathrm{Hg}}_{\mathrm{m}\infty}}{(1/\tau^{\mathrm{Hg^m}}) + n_\mathrm{e}(S^{\mathrm{Hg}}_{\mathrm{m}\infty} + \bar{S}^{\mathrm{Hg}}_{\mathrm{m}0})} \right) \cdot \tau^{\mathrm{Hg^+}}_{\mathrm{diff}} \cdot \tag{38}$$

In accordance with[40,41], the direct ionization of Hg can be neglected against the stepwise ionization for discharge currents higher than 40 mA. Since on the other hand the mass spectrometric measured ion effusion currents $i(\mathrm{Hg^+})$ are increasing linearly with i_d or n_e respectively, the $\mathrm{Hg^+}$-formation must take place via $\mathrm{Hg^m}$, which for his part does not vary with i_d. Population and depopulation of $\mathrm{Hg^m}$ by electron collisions are in equilibrium. The optical measurements by Koedam and Kruithof[36] show, that $\mathrm{Hg}(^3\mathrm{P}_0)$ and $\mathrm{Hg}(^3\mathrm{P}_2)$ do not vary with the discharge current for $i_\mathrm{d} > 40$ mA. Thus, for discharge currents $i_\mathrm{d} > 40$ mA we have

$$[\mathrm{Hg^+}] = n_\mathrm{e}[\mathrm{Hg}] \cdot \frac{S^{\mathrm{Hg}}_{0\mathrm{m}} \cdot S^{\mathrm{Hg}}_{\mathrm{m}\infty}}{(S^{\mathrm{Hg}}_{\mathrm{m}\infty} + \bar{S}^{\mathrm{Hg}}_{\mathrm{m}0})} \cdot \tau^{\mathrm{Hg^+}}_{\mathrm{diff}}\,. \tag{39}$$

Neglecting the direct ionization of argon against the stepwise ionization, we find for $i_\mathrm{d} > 40$ mA the relations

$$\frac{[\mathrm{Ar^+}]}{[\mathrm{Hg^+}]} = \frac{[\mathrm{Ar}]}{[\mathrm{Hg}]} \cdot n_\mathrm{e} \cdot \frac{S^{\mathrm{Ar}}_{0\mathrm{m}} \cdot S^{\mathrm{Ar}}_{\mathrm{m}\infty} \cdot (S^{\mathrm{Hg}}_{\mathrm{m}\infty} + \bar{S}^{\mathrm{Hg}}_{\mathrm{m}0})}{([1/\tau^{\mathrm{Ar^m}}) + [\mathrm{Hg}] \cdot k^{\mathrm{ArHg^+}} + n_\mathrm{e} \cdot (S^{\mathrm{Ar}}_{\mathrm{m}\infty} + \bar{S}^{\mathrm{Ar}}_{\mathrm{m}0})]\, S^{\mathrm{Hg}}_{0\mathrm{m}} \cdot S^{\mathrm{Hg}}_{\mathrm{m}\infty}} \cdot \frac{\tau^{\mathrm{Ar^+}}_{\mathrm{diff}}}{\tau^{\mathrm{Hg^+}}_{\mathrm{diff}}} \tag{40}$$

and

$$\frac{[\mathrm{Ar_2^+}]}{[\mathrm{Ar^+}]} = \frac{1}{n_\mathrm{e}} \cdot \frac{\tau^{\mathrm{Ar^*}} \cdot k^{\mathrm{Ar_2^+}} \cdot [\mathrm{Ar}]}{1 + \tau^{\mathrm{Ar^*}} \cdot k^{\mathrm{Ar_2^+}} \cdot [\mathrm{Ar}]} \cdot \frac{S^{\mathrm{Ar}}_{0*}}{S^{\mathrm{Ar}}_{0\mathrm{m}} \cdot S^{\mathrm{Ar}}_{\mathrm{m}\infty}} \cdot ((1/\tau^{\mathrm{Ar^m}}) + k^{\mathrm{ArHg^+}} \cdot [\mathrm{Hg}] + n_\mathrm{e}(S^{\mathrm{Ar}}_{\mathrm{m}\infty} + \bar{S}^{\mathrm{Ar}}_{\mathrm{m}0})) \cdot \frac{\tau^{\mathrm{Ar_2^+}}_{\mathrm{diff}}}{\tau^{\mathrm{Ar^+}}_{\mathrm{diff}}}\,. \tag{41}$$

For $[\mathrm{ArHg^+}]/[\mathrm{Ar_2^+}]$ we get from (23)

$$\frac{[\mathrm{ArHg^+}]}{[\mathrm{Ar_2^+}]} = \frac{S^{\mathrm{Ar}}_{0\mathrm{m}}}{S^{\mathrm{Ar}}_{0*}} \cdot \frac{\tau^{\mathrm{Ar^m}} \cdot k^{\mathrm{ArHg^+}} \cdot [\mathrm{Hg}]}{1 + \tau^{\mathrm{Ar^m}} \cdot k^{\mathrm{ArHg^+}} \cdot [\mathrm{Hg}]} \cdot \frac{1 + \tau^{\mathrm{Ar^*}} \cdot k^{\mathrm{Ar_2^+}} \cdot [\mathrm{Ar}]}{\tau^{\mathrm{Ar^*}} \cdot k^{\mathrm{Ar_2^+}} \cdot [\mathrm{Ar}]} \cdot \frac{\tau^{\mathrm{ArHg^+}}_{\mathrm{diff}}}{\tau^{\mathrm{Ar_2^+}}_{\mathrm{diff}}}\,. \tag{42}$$

With the Eqs. (40), (41), (42), the results of Fig. 2 can now be discussed.

According to (42), the ratio $\mathrm{ArHg^+}/\mathrm{Ar_2^+}$ is proportional to p_Hg, if $\tau^{\mathrm{Ar^m}} \cdot k^{\mathrm{ArHg^+}} \cdot [\mathrm{Hg}] \ll 1$ or correspondingly if $p_\mathrm{Hg} < 5 \cdot 10^{-3}$ torr. As seen in Fig. 2, the proportionality with p_Hg is observed in this pressure range.

According to (40), $[\mathrm{Ar^+}]/[\mathrm{Hg^+}]$ must be inversely proportional to p_Hg, if n_e is nearly constant. As n_e does not vary strongly with p_Hg (see [33,34]), this reciprocal relationship is fulfilled in Figure 2.

The ratio $[\mathrm{Ar_2^+}]/[\mathrm{Ar^+}]$ is found in Fig. 2 nearly independent on p_Hg. This result agrees with Equation (41). Here $[\mathrm{Ar_2^+}]/[\mathrm{Ar^+}]$ is not dependent on p_Hg as long as the depopulation of $\mathrm{Ar^m}$ by the $\mathrm{ArHg^+}$-formation can be neglected against the other depopulation processes.

Concerning the dependence of the ion current ratios $i(\mathrm{ArHg^+})/i(\mathrm{Ar_2^+})$, $i(\mathrm{Ar^+})/i(\mathrm{Hg^+})$ and $i(\mathrm{Ar_2^+})/i(\mathrm{Ar^+})$ on the discharge current, there is a fair agreement between the experiment and the Eqs. (42), (40) and (41): $[\mathrm{ArHg^+}]/[\mathrm{Ar_2^+}]$ is nearly independent on i_d. $[\mathrm{Ar^+}]/[\mathrm{Hg^+}]$ is proportional to i_d and $[\mathrm{Ar_2^+}]/[\mathrm{Ar^+}]$ is inversely proportional to i_d.

Concerning the variation of the ion current ratios with p_Ar, $[\mathrm{ArHg^+}]/[\mathrm{Ar_2^+}]$ should be inversely proportional to p_Ar (see (42)), if $\tau^{\mathrm{Ar^*}} \cdot k^{\mathrm{Ar_2^+}} \cdot [\mathrm{Ar}] \ll 1$, or correspondingly, if $p_\mathrm{Ar} < 0.2$ torr. Actually, the ratio $i(\mathrm{ArHg^+})/i(\mathrm{Ar_2^+})$ is varying slowly with p_Ar in this pressure range. This behavior may be explained as follows: According to [33,34] the electron temperature T_e is increasing strongly with decreasing argon pressure. With regard to the great difference of the excitation energies of the $\mathrm{Ar^m}$ (11.5 eV) and of Ar (14.7 eV), in (42) the collision rate S^{Ar}_{0*} will increase strongly as compared to $S^{\mathrm{Ar}}_{0\mathrm{m}}$. Therefore the ratio $[\mathrm{ArHg^+}]/[\mathrm{Ar_2^+}]$ will not increase with $1/p_\mathrm{Ar}$ in direction of lower argon pressures.

A similar explanation seems to be valid for the measured $i(\mathrm{Ar^+})/i(\mathrm{Hg^+})$ ratio as a function of p_Ar: Lower argon pressure effects higher electron temperature. Therefore, the stepwise ionization of argon is

highly favored against the stepwise ionization of Hg, so that the Ar^+-concentration is increasing with respect to the Hg^+-concentration if p_{Ar} is diminished.

The $ArHg^+$-formation process certainly is in concurrence with the process of Penning-ionization:

$$Ar^m + Hg \rightarrow Ar + Hg^+ + e\,, \qquad (42)$$

which also is exothermal according to Figure 3. If we compare our cross section for the $ArHg^+$-formation, $\sigma = 5.8 \cdot 10^{-15}$ cm², with the cross section of the Penning-ionization measured by Pfau and Rutscher[42] for the mercury-neon system, $\sigma = 3.7 \cdot 10^{-15}$ cm², we find that both cross sections are nearly the same. Thus we must suppose, that the Penning effect which generally is made responsible for the breakdown of a Hg-Ar-discharge, must be replaced in a great measure by the $ArHg^+$-formation (12).

With our $\tau^{Ar^*} \cdot k^{Ar_2^+}$-value (32), from (23) and Fig. 4 the ratio of the excitation rates S_{0*}^{Ar} and S_{0m}^{Ar} can be evaluated. The ratio of the diffusion lifetimes of Ar_2^+ and $ArHg^+$, which must be known for this determination, is found from the ratio of ion-mobilities calculated from[43]. So we get

$$b_+(Ar_2^+)/b_+(ArHg^+) = 1.28 \text{ and}$$
$$S_{0*}^{Ar}/S_{0m}^{Ar} = 0.09\,. \qquad (43)$$

In the same way, the ratio of the ionization rate $S_{0\infty}^{Ar}$ and excitation rate can be determined from (31) and Figure 5. We find

$$S_{0\infty}^{Ar}/S_{0*}^{Ar} = 2.1\,.$$

This result can be understood by the fact, that the ionization cross section of Ar is much greater than the electronic excitation cross sections (see e.g.[44]).

We wish to acknowledge the useful technical assistance of H. Lüdemann.

[1] G. Franck and H. Lüdemann, Z. Naturforsch. **27 a**, 1278 [1972].
[2] R. Fuchs and W. Kaul, Z. Naturforsch. **15 a**, 108 [1960].
[3] W. Kaul and R. Fuchs, Z. Naturforsch. **15 a**, 326 [1960].
[4] J. S. Dahler, J. L. Franklin, M. S. B. Munson, and F. H. Field, J. Chem. Phys. **36**, 3332 [1962].
[5] H. V. Koch and L. Friedman, J. Chem. Phys. **38**, 1115 [1963].
[6] C. E. Melton and W. Hamill, J. Chem. Phys. **41**, 1469 [1964].
[7] P. M. Becker and F. W. Lampe, J. Chem. Phys. **42**, 3857 [1965].
[8] W. A. Chupka and M. E. Russell, J. Chem. Phys. **49**, 5426 [1968].
[9] J. J. De Carpo and F. W. Lampe, J. Chem. Phys. **51**, 943 [1969].
[10] M. Pahl and U. Weimer, Z. Naturforsch. **13 a**, 745 [1958].
[11] M. Pahl, Z. Naturforsch. **14 a**, 239 [1959].
[12] P. F. Knewstubb and A. W. Tickner, J. Chem. Phys. **36**, 674 [1962].
[13] P. F. Knewstubb and A. W. Tickner, J. Chem. Phys. **36**, 684 [1962].
[14] J. A. Hornbeck and J. P. Molnar, Phys. Rev. **84**, 621 [1951].
[15] M. Pahl and U. Weimer, Z. Naturforsch. **12 a**, 926 [1957].
[16] W. Kaul, U. Lauterbach, and R. Fuchs, Naturwiss. **47**, 353 [1960].
[17] P. Kebarle, R. M. Haynes, and S. K. Searles, J. Chem. Phys. **47**, 1684 [1967].
[18] M. Pahl, Z. Naturforsch. **18 a**, 1276 [1963].
[19] D. P. Stevenson and D. O. Schissler, J. Chem. Phys. **29**, 282 [1958].
[20] D. P. Stevenson and D. O. Schissler, J. Phys. Chem. **61**, 1453 [1957].
[21] J. B. Ortenburger, M. Herzberg, and R. A. Ogg, J. Chem. Phys. **33**, 579 [1960].
[22] M. Herzberg, D. Rapp, J. B. Ortenburger, and D. D. Braglia, J. Chem. Phys. **34**, 343 [1961].
[23] W. Kaul, U. Lauterbach, and R. Taubert, Z. Naturforsch. **16 a**, 624 [1961].
[24] C. F. Giese and W. B. Maier, J. Chem. Phys. **35**, 1913 [1961].
[25] T. F. Moran and L. Friedman, J. Chem. Phys. **39**, 2491 [1963].
[26] V. Aquilanti, A. Galli, A. Giardini-Guidoni, and G. G. Volpi, J. Chem. Phys. **43**, 1969 [1965].
[27] M. A. Berta, B. Y. Ellis, and W. S. Koski, J. Chem. Phys. **44**, 4612 [1966].
[28] W. A. Chupka and M. E. Russell, J. Chem. Phys. **49**, 5426 [1968].
[29] J. L. Gilkinson, H. Held, and L. M. Chanin, J. Appl. Phys. **40**, 2350 [1969].
[30] Z. Herman and V. Čermák, Nature (London) **199**, 588 [1963]. Coll. Czech. Chem. Commun. **28**, 799 [1963].
[31] M. S. B. Munson, F. H. Field, and J. L. Franklin, J. Chem. Phys. **37**, 1790 [1962].
[32] A. Henglein and G. A. Muccini, Z. Naturforsch. **15 a**, 584 [1960].
[33] W. Verwey, Philips Res. Rep. Suppl., Nr. 2 [1960].
[34] W. Verwey, Physica **25**, 980 [1959].
[35] K. Wojaczek, Beitr. Plasmaphys. **5**, 307 [1965].
[36] M. Koedam and A. A. Kruithof, Physica **28**, 80 [1962].
[37] G. Herzberg, Molecular Spectra and Molecular Structure, I. Spectra of Diatomic Molecules, D. van Nostrand Comp., Inc. 1961.
[38] R. E. Huffman and H. Katayama, J. Chem. Phys. **45**, 138 [1966].
[39] Landolt-Börnstein, Zahlenwerte und Funktionen, Verlag Springer, Berlin-Göttingen-Heidelberg 1950, Bd. I, 1. Teil, S. 326.
[40] M. A. Cayless, Brit. J. Appl. Phys. **10**, 186 [1959].
[41] J. Polman and P. C. Drop, J. Appl. Phys. **43**, 1577 [1972].
[42] S. Pfau and A. Rutscher, Ann. Phys. **25**, 321 [1970].
[43] H. S. W. Massey, Electronic and Ionic Impact Phenomena, Vol. III, At the Clarendon Press, Oxford 1971, p. 1959.
[44] P. Laborie, J.-M. Rocard, and J. A. Rees, Electronic Cross Sections, 1 — Hydrogen and Rare gases, Dunod 1968.